Polymer Blends of Poly(trimethylene terephthalate) and Polystyrene Compatibilized by Styrene-Glycidyl Methacrylate Copolymers

Jieh-Ming Huang*

Department of Chemical Engineering, Van Nung Institute of Technology, 1, Van Nung Road, Chung-Li City, Taiwan 320, Republic of China

Received 27 May 2002; accepted 27 August 2002

ABSTRACT: The compatibilizing effects of styrene-glycidyl methacrylate (SG) copolymers with various glycidyl methyacrylate (GMA) contents on immiscible blends of poly(trimethylene terephthalate) (PTT) and polystyrene (PS) were investigated using scanning electron microscopy (SEM), Fourier transform infrared spectroscopy (FTIR), and ^{13}C-solid-state nuclear magnetic resonance (NMR) spectroscopy. The epoxy functional groups in the SG copolymer were able to react with the PTT end groups (—COOH or —OH) to form SG-*g*-PTT copolymers during melt processing. These *in situ*–formed graft copolymers tended to reside along the interface to reduce the interfacial tension and to increase the interfacial adhesion. The compatibilized PTT/PS blend possessed a smaller phase domain, higher viscosity, and better tensile properties than did the corresponding uncompatibilized blend. For all compositions, about 5% GMA in SG copolymer was found to be the optimum content to produce the best compatibilization of the blend. This study demonstrated that SG copolymers can be used efficiently in compatibilizing polymer blends of PTT and PS. © 2003 Wiley Periodicals, Inc. J Appl Polym Sci 88: 2247–2252, 2003

Key words: poly(trimethylene terephthalate); polystyrene; polymer blend; compatibilization; solid-state NMR

INTRODUCTION

Poly(trimethylene terephthalate) (PTT), which has three methylene moieties in its backbone, is an aromatic polyester. Of the polymers in the aromatic homologous series, both poly(ethylene terephthalate) (PET) and poly(butylene terephthalate) (PBT) have been studied thoroughly during the last decade.[1–8] PTT has been of interest only recently because one of its raw materials, 1,3-propanediol, was unavailable until Shell Chemical Company discovered a low-cost monomer process in 1997.[9] Because of its outstanding resilience, relatively low melting temperature, and ability to rapidly crystallize, PTT offers potential opportunity for use in carpet, textile, and thermoplastic applications. In recent years many studies on PTT such as synthetic techniques[10–12] and morphological structure,[13,14] as well as crystallization kinetics,[15,16] have been investigated extensively. However, there have been relatively few studies on polymer blends composed of PTT with other polymers.[17,18]

Polystyrene (PS) is a low-cost commodity polymer with unique properties. Because of the intrinsically different structures of PTT and PS, it has been expected that PTT/PS blends would be immiscible and incompatible. For blends of polymers containing functional groups, reactive compatibilization may be a good method to improve compatibility.[19–21] During the process of melt blending, a portion of the reactive compatibilizer has the chance to locate in the vicinity of the interface and to react with the other component to form graft or block copolymers. Consequently, these *in situ*–formed copolymers tend to anchor and concentrate at the interface to serve as effective compatibilizers between two immiscible polymers. Therefore, the performance of a compatibilized blend can be improved as a result of the enhanced interface adhesion in the solid state. Furthermore, compatibilizing an incompatible blend usually results in finer and more stable morphology, better processibility, and improved mechanical properties. In previous studies we employed the styrene-glycidyl methacrylate (SG) copolymer as the *in situ* compatibilizer for both PET/PS and PBT/PS blends.[22,23] In this study we used SG copolymers with various GMA contents to compatibilize the PTT/PS blends, focusing on investigating their specific miscibility and correlating it with their morphology, interaction, and mechanical properties.

*E-mail: jiehming@cc.vit.edu.tw.

Contract grant sponsor: National Science Council, Taiwan, Republic of China; contract grant number: NSC-90-2216-E-238-001.

Contract grant sponsor: Van Nung Institute of Technology.

Journal of Applied Polymer Science, Vol. 88, 2247–2252 (2003)

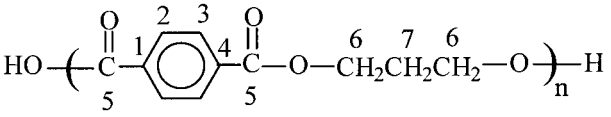

Poly(trimethylene terephthalete) (PTT)

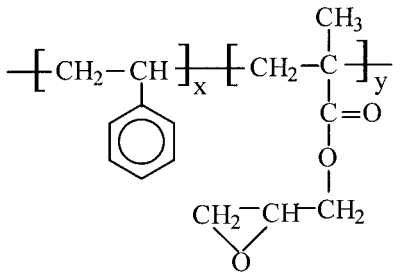

Styrene-glycidyl methacrylate copolymers (SG)

Figure 1 Chemical structures of PTT and SG and atom-numbering schemes.

EXPERIMENTAL

Materials

PTT with I.V. = 0.66 was kindly supplied by Shinkong Co. of Taiwan. Polystyrene, PG-33, was purchased from Chi-Mei Co. of Taiwan. Styrene-glycidyl methacrylate copolymers containing varied glycidyl methacrylate contents were prepared by suspension polymerization. The detailed procedures were previously described.[22] The chemical structures of PTT and SG are illustrated in Figure 1.

Melt blending and specimen preparation

All blends were prepared in a 30-mm corotating twin-screw extruder with an L/D of 36, a barrel temperature ranging from 230°C to 250°C, and a screw speed of 250 rpm. The extruded pellets were dried at 90°C for more than 12 h and then molded into standard ASTM specimens by using an Arburg 3-oz injection molding machine (Lossburg, Germany).

Characterizations

Melt flow rates of the base polymers and their blends were measured at 250°C using a load of 2.16 kg by an automatic flow-rate timer from Ray-Ran Corp. (UK). Morphologies of the cryogenically fractured surfaces of the injection-molded specimens were examined by scanning electron microscopy (SEM) using a model S-570 from Hitachi Corp. of Japan. Standard tensile tests were conducted following the ASTM D-638 method at ambient conditions with a crosshead speed of 5 mm/min. Infrared spectra were recorded on a Perkin-Elmer spectra-one infrared spectroscopy. All the spectra were scanned at a resolution of 2 cm^{-1}, and 32 scans were collected.

High-resolution solid-state ^{13}C-NMR experiments were carried out at room temperature using a Bruker DSX-400 spectrometer operated at resonance frequencies of 399.53 and 100.47 MHz for ^{1}H and ^{13}C, respectively. The ^{13}C-CP/MAS NMR spectra were measured with a 3.9-μs 90° pulse, with a 5-s pulse delay time, an acquisition time of 30 ms; 1024 scans were accumulated. All NMR spectra were taken at 300 K using broadband proton decoupling and a normal cross-polarization pulse sequence. A magic-angle spinning (MAS) rate of 5.4 kHz was used to eliminate resonance broadening from the anisotropy of the chemical shift tensors. The proton spin-lattice relaxation time in the rotating frame ($T_{1\rho}{}^{H}$) was measured indirectly via carbon observation using a 90°-τ-spin lock pulse sequence prior to cross-polarization. Data acquisition was performed with ^{1}H decoupling and a delay time (τ) ranging from 0.2 to 24 ms, with a contact time of 1.0 ms.

RESULTS AND DISCUSSION

Melt flow rate

The melt flow rate (MFR) is an inverse function of viscosity and can be used to assess the interaction between the phases. From Table I, which summarizes the melt flow rates of PTT, PS, and the PTT/PS blends, it is evident that PTT had a higher MFR than did the PS in the tested conditions, and the blend showed a decrease in MFR after compatibilization. Furthermore, the SG copolymer with a higher GMA content resulted in a lower MFR than did the corresponding SG with a

TABLE I
Melt Flow Rates and Tensile Strength of PTT/PS Blends

Composition	MFR[a] (g/10 min)	Tensile strength (MPa)
PTT	99.8	55.8
PS	16.1	35.3
PTT/PS = 75:25	71.6	45.8
PTT/PS/SG2 = 75:25:5	50.1	50.1
PTT/PS/SG5 = 75:25:5	46.0	53.6
PTT/PS/SG10 = 75:25:5	43.4	52.1
PTT/PS = 50:50	48.3	39.3
PTT/PS/SG2 = 50:50:5	26.7	45.5
PTT/PS/SG5 = 50:50:5	20.6	48.8
PTT/PS/SG10 = 50:50:5	16.8	46.9
PTT/PS = 25:75	53.7	33.6
PTT/PS/SG2 = 25:75:5	42.6	38.2
PTT/PS/SG5 = 25:75:5	29.4	41.0
PTT/PS/SG10 = 25:75:5	18.6	38.6

[a] Tested at 250°C with a load of 2.16 kg

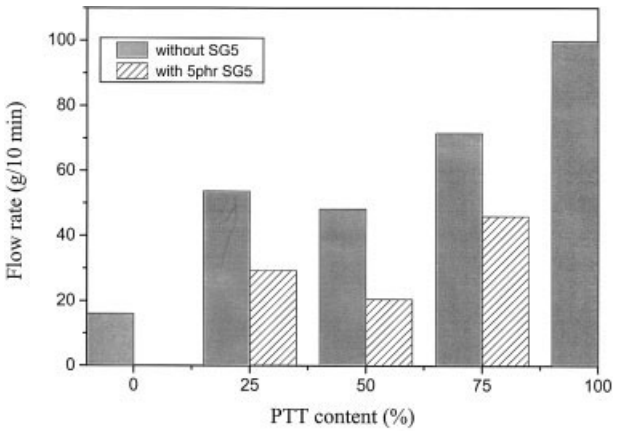

Figure 2 Effect of SG5 on melt flow rate for PTT/PS blends.

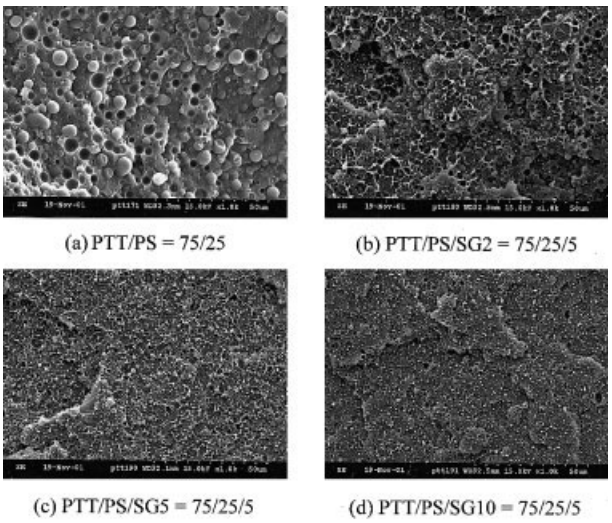

Figure 3 SEM micrographs of the cryogenic fractured surfaces for the compatibilized and uncompatibilized PTT/PS (75:25) blends.

lower GMA content. It has been reported that the SG copolymer can act as a reactive compatibilizer for PET and PS blends.[22] Therefore, the epoxy groups in the SG copolymer also are able to react with PTT end groups (—COOH or —OH) to form SG-*graft*-PTT copolymers during melt processing. The molecular increase through the grafting reaction is believed to be the major contribution to the viscosity increase of the blend. These *in situ*–formed SG-*g*-PTT copolymers tend to concentrate at the interface and therefore raise the interfacial friction under shear stress. The increased interfacial friction of the compatibilized blend over that of the uncompatibilized one is another reason for the observed higher viscosity. This explains why the greatest viscosity drop occurred in the blend when both phases were in a cocontinuous structure (PTT/PS = 50:50), as shown in Figure 2.

Scanning electron microscopy

Figure 3 shows the scanning electron microscopy (SEM) micrographs of the cryogenic fracture surfaces without solvent etching for the compatibilized and noncompatibilized PTT/PS = 75:25 blends. The large dispersed and spherical PS particles with different dimensions (5–10 μm) can be easily identified from the noncompatibilized blend, as shown in Figure 3(a). Compared with that of the noncompatibilized blends [Figure 3(a,b)], the domain size of the PS particles decreased when the SG2 compatibilizer was added to the blend. It is evident that the blends whose SG copolymers had a higher GMA content [Figs. 3(c,d)] resulted in finer phase domains (0.5–3 μm). Figure 4 shows SEM micrographs of the cryogenically fractured surfaces of the PTT/PS blends after solvent etching. In Figure 4 the PS particles being etched out by tetrahydrofuran are the empty holes, which were significantly large for the uncompatibilized PTT/PS = 75:25 blend. The domain size decreased after 5 phr of the SG compatibilizer was added to the blend. This observed trend is very similar to the previous melt flow rate in terms of the presence of SG; the better compatibilized blend had a higher viscosity and exhibited a smaller domain size. This was because of the *in situ*–formed compatibilizer reducing the interfacial tension during melt blending, resulting in a finer domain size of the dispersed-phase particles. Figure 5 shows the surface morphologies of the PTT/PS = 50:50 blends after solvent etching. Compared with the domain sizes shown in Figure 4(a) and Figure 5(a), the domain size of the holes was larger for the blend containing a higher PS content in the blend, as would be expected. The domains became smaller and irregular when SG2 compatibilizer was added to the blend, as shown in Figure 5(b). Moreover, there was a signif-

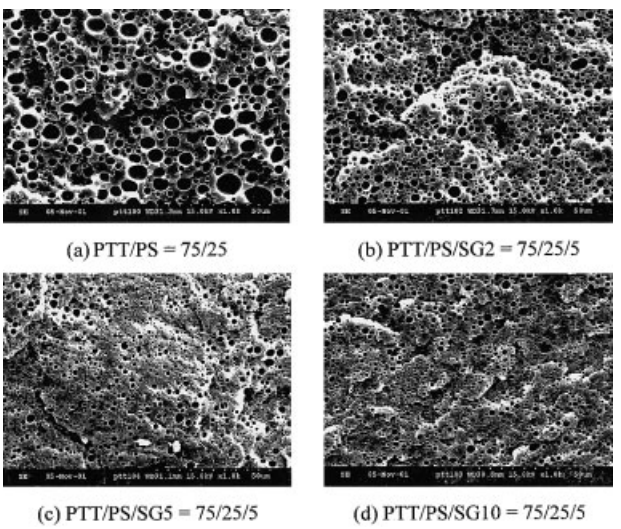

Figure 4 SEM micrographs of the etched cryogenic surfaces for the compatibilized and uncompatibilized PTT/PS (75:25) blends.

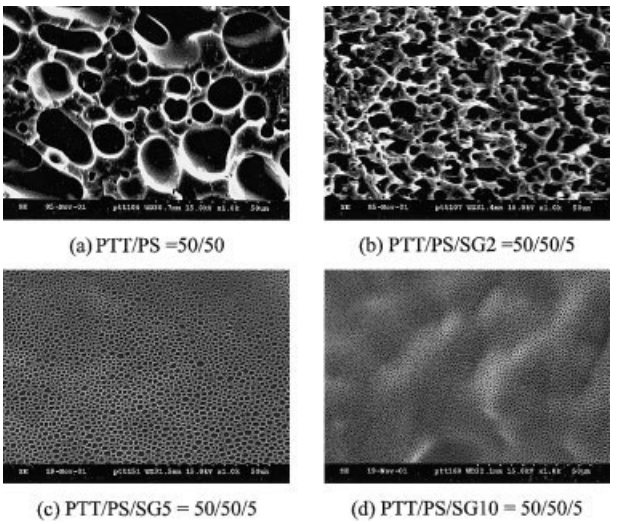

Figure 5 SEM micrographs of the etched cryogenic surfaces for the compatibilized and uncompatibilized PTT/PS (50:50) blends.

icant decrease in domain size for the blend with 10 phr of GMA in the SG copolymer [Fig. 5(d)]. The trend is clear that a higher GMA content in SG results in a smaller domain size in the blend.

Mechanical properties

Figure 6 compares the tensile strength of the PTT/PS blends with and without 5 phr SG5, and the detailed data are summarized in Table I. It is evident that blends with SG5 compatibilizer exhibited higher tensile strength for all compositions. Figure 7 shows the tensile strength of the blends as a function of GMA content in the SG copolymers for various PTT/PS composition ratios. The trend is for the blend with a higher PTT content to show a higher tensile strength. Furthermore, the presence of 5% GMA in the SG copolymer exhibited the highest tensile strength in all

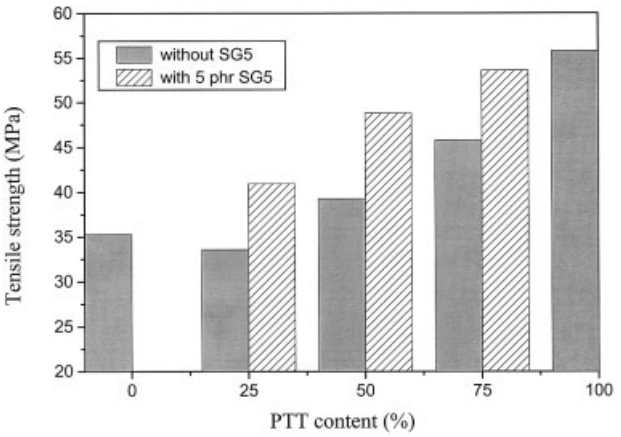

Figure 6 Effect of SG5 on tensile strength of PTT/PS blends.

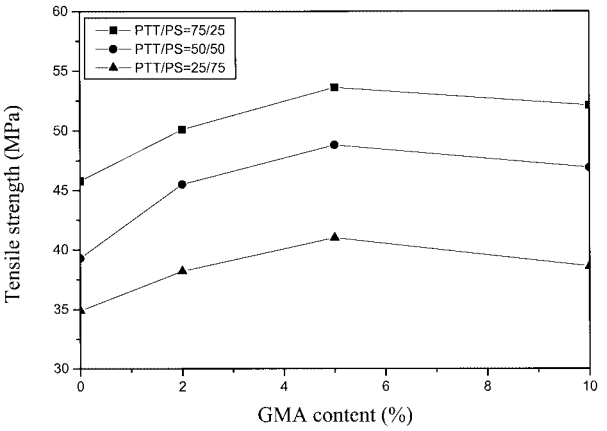

Figure 7 Effect of GMA content in SG copolymers on tensile strength of PTT/PS blends.

compositions. As reported previously,[24] a higher GMA content in SG may produce an excessively grafted copolymer, which is considered a less effective compatibilizer. An SG copolymer with a lower GMA content has the advantage of producing lightly grafted copolymers; but it also has the tendency to produce fewer numbers of grafted copolymers.

Fourier transform infrared spectroscopy analyses

Infrared spectroscopy has become a powerful tool to study polymer blend miscibility. If the blend is totally immiscible, the absorption spectrum of the blend will be the sum of those for the components. If the blend is miscible or partially miscible, specific interactions between the two components perturbs the bonding between atoms, and differences will be seen in the spectrum of the blend when compared with the sum of those for the components. Figure 8 shows the infrared spectra measured at 25°C as ranging from 800 to 1200 cm^{-1} for SG5, powder-blended, and melt-blended

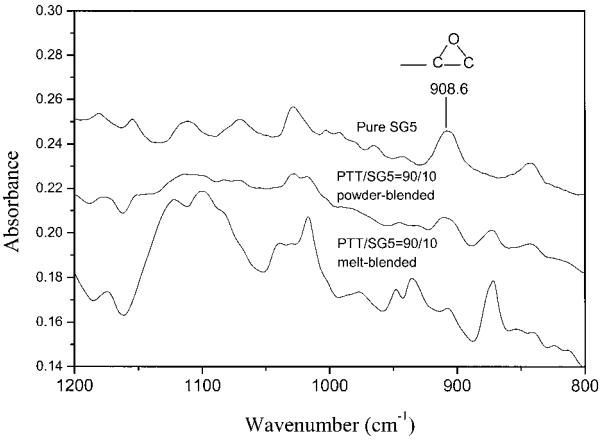

Figure 8 FTIR spectra in the 1200–800 cm^{-1} region for SG5, powder-blended, and melt-blended PTT/PS (90:10) blends.

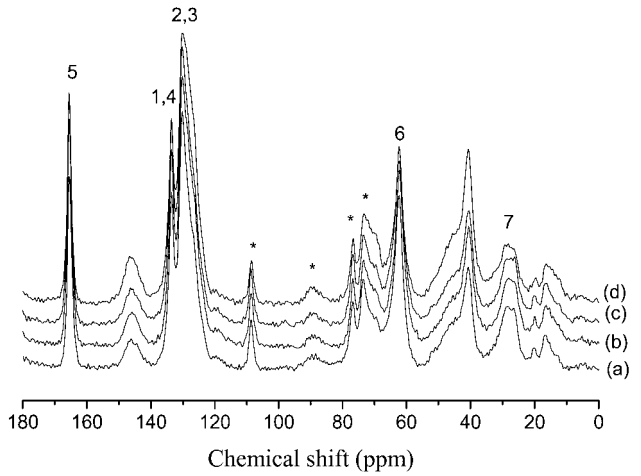

Figure 9 ^{13}C-CP/MAS spectra of PTT/PS blends: (a) PTT/PS (75:25); (b) PTT/PS/SG2 (75:25:5); (c) PTT/PS/SG5 (75:25:5); (d) PTT/PS/SG10 (75:25;5) [asterisks denote spinning sidebands].

PTT/SG5 (90:10) blends. The characteristic epoxy peak (908.6 cm^{-1}) of the melt-blended sample is significantly smaller than that of its powder-blended counterpart. This can be attributed to the reaction between the epoxy group of the SG5 with the carboxylic acid and hydroxyl end groups of the PTT. Because the reduction of the observed epoxy peak does not account for all the epoxy groups consumed in the reaction, epoxy hydrolysis or other unknown reactions may also be involved.[22]

^{13}C-CP/MAS NMR spectra

Solid-state NMR spectroscopy provides further insight into the phase behavior and morphology of polymer blends.[25,26] The ^{13}C-CP/MAS spectra of the PTT/PS (75:25) blends are shown in Figure 9, and the peak assignments are shown in Figure 1. The combination of dipolar decoupling and magic-angle spinning (MAS) resulted in a sufficiently high resolution to resolve the carbonyl carbon (δ_0 = 165.5 ppm), aromatic carbons (130.2, 133.5 ppm), and methylene carbons (62.3, 28.4 ppm). In Figure 9 it can be seen that the ^{13}C-NMR peaks are well resolved, allowing for a clear estimation of $T_{1\rho}{}^H$ and the peak width of the respective moieties in the blends. The resonance width of the aromatic carbons (C_2, C_3) increased with increasing GMA content in the SG copolymer, as shown in Figure 9. It is evident that the broadening of the peak width originated from the inhomogeneity of the structure, caused by the addition of SG copolymers to the blend. The structural inhomogeneity gave rise to a distribution of the chemical shifts from the parent polymers, leading to broadening of the NMR absorption lines.

Proton spin-lattice relaxation ($T_{1\rho}{}^H$) analyses

The proton spin-lattice relaxation time in the rotating frame, $T_{1\rho}{}^H$, has been used widely to examine inhomogeneity of domains. A proton, $T_{1\rho}{}^H$, via resolved carbon resonance provides a convenient method to access the complicated morphology of polymer blends and to characterize molecular motion in polymers.[27–30] $T_{1\rho}{}^H$ can be observed for protons in different morphological domains. The spin diffusion is weak and can be neglected, provided that the coupled domain is large enough. The normalized ^{1}H-magnetization [M(τ)] of PTT is simulated by the double-exponential function, which reflects the two relaxation rates of both domains as follow:

$$M(\tau)/M(0) = x_a \exp(-\tau/T_{1\rho}{}^H{}_{,S}) + x_c \exp(-\tau/T_{1\rho}{}^H{}_{,L}) \quad (1)$$

where $T_{1\rho}{}^H{}_{,S}$ and $T_{1\rho}{}^H{}_{,L}$ correspond to the relaxation times in the mobile and rigid components and x_a and x_c are the respective weight fractions of the domain. The value of $T_{1\rho}{}^H$ can be obtained from the slope of the plot of ln [$M(\tau)/M(0)$] versus spin lock time. Biexponential decay is apparent from Figure 10, which shows the magnetization decay curves of C_5 (165.5 ppm) as a function of spin lock time for the PTT/PS (75:25) and PTT/PS/SG10 (75:25:5) blends. This biexponential decay corresponds to the relaxation of PTT protons in the more mobile (short time component) and the more rigid (long time component) regions. The $T_{1\rho}{}^H$ values obtained from the carbonyl carbon (165.5 ppm) are summarized in Table II. It is obvious that the $T_{1\rho}{}^H$ values of the PTT/PS (75:25) blend are greater than those of the PTT. Furthermore, the fraction of the long time component decreased when the PS was added to the PTT. Adding SG10 to the blend also resulted in a longer relaxation time (larger $T_{1\rho}{}^H$ value), implying

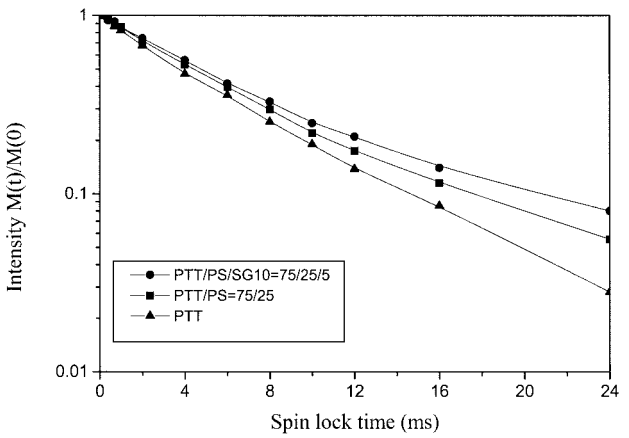

Figure 10 Semilogarithmic plots of the magnetization intensity of 165.5 ppm carbonyl as a function of spin-lock time for PTT, PTT/PS (75:25), and PTT/PS/SG10 (75:25:5) blends.

TABLE II
$T_{1\rho}{}^{H}$ values of 165.5 ppm for PTT and PTT/PS Blends

Composition	$T_{1\rho}{}^{H}$ (ms)	
	Short time component	Long time component
PTT	1.20 (19.1%)[a]	6.71 (80.9%)
PTT/PS = 75:25	2.68 (29.6%)	8.24 (70.4%)
PTT/PS/SG10 = 75:25:5	3.32 (40.6%)	10.04 (59.4%)

[a] The value in parentheses represents the weight fraction of the respective component.

that the proton relaxes more slowly and that molecular mobility is more rigid when the PTT/PS blend contains 5 phr SG 10. These *in situ*–formed PTT-*g*-SG copolymers tended to restrict the segmental motion of polymer chains and cause a longer relaxation time than those of the PTT/PS blend. Table II shows that the fraction of the long time component (rigid region) of the compatibilized PTT/PS/SG10 blend was lower than that of the uncompatibilized PTT/PS blend. The formation of these PTT-*g*-SG copolymers leads to lower PTT crystallinity. These *in situ*–formed graft copolymers can serve as interfacial compatibilizers between the PTT and PS, enhancing its miscibility.

CONCLUSIONS

Polymer blends of PTT and PS are immiscible and incompatible, with poor interfacial adhesion and large phase domains. Epoxy groups in SG copolymers are able to react with PTT end groups to form various SG-*graft*-PTT copolymers, which tend to concentrate at the interface to compatibilize PTT/PS blends. The improvement in tensile strength of the compatibilized blends can be attributed to the expected improvement in interfacial adhesion. The lightly grafted SG-*g*-copolymer is considered a more effective compatibilizer than the excessively grafted one. The better-compatibilized blend shows a finer phase dispersion, better processibility, improved mechanical properties, and great morphological stability. Solid-state NMR spectra show a biexponential decay of the PTT component. The SG10 compatibilized blend possesses a greater $T_{1\rho}{}^{H}$ value, but there is a decreased fraction of the long time component (the more rigid region). These PTT-*g*-SG copolymers reside at the interface and tend to restrict the segmental motion of the polymer chains, resulting in smaller PTT crystalline domains.

References

1. Roberts, R. C. Polymer 1969, 10, 113.
2. Sefcik, M. D.; Schaefer, J.; Stejskal, E. O.; Mckay, R. A. Macromolecules 1980, 13, 1132.
3. Goschel, U. Polymer 1996, 37, 4049.
4. Nealy, D. L.; Davis, T. G.; Kibler, C. J. J Polym Sci A-2, 1970, 8, 2141.
5. Fakirov, S.; Fischer, E. W.; Hoffmann. R.; Schmidt, G. Polymer 1977, 18, 1121.
6. Nichols, M. E.; Robertson, R. E. J Polym Sci, Polym Phys Ed 1992, 30, 755.
7. Cole, K. C.; Ajji, A.; Pellerin, E. Macromolecules 2002, 35, 770.
8. Kim, H. G.; Robertson, R. E. J Polym Sci, Polym Phys Ed 1998, 36, 1757.
9. Dangayach, K.; Chuah, H.; Gergen, W.; Dalton, P.; Smith, F. Plastics—Saving Planet Earth, 55th ANTEC Proceedings 2097, 1997.
10. Ng, T. H.; Williams, H. L. Makromol Chem 1981, 182, 3323.
11. Gonzalez, C. C.; Perena, J. M.; Bello, A. J Polym Sci Polym, Phys Ed 1988, 26, 1397.
12. Imamura, T.; Sato, T.; Matsumoto, T. Jpn. Pat. 8,232,117 (1996).
13. Peres, S.; Suzie, P. D.; Revol, J. F.; Brisse, F. Polymer 1979, 20, 419.
14. Wu, J.; Schultz, J. M.; Samon, J. M.; Pangelinan, A. B.; Chuah, H. H. Polymer 2001, 42, 7141.
15. Huang, J. M.; Chang, F. C. J Polym Sci, Polym Phys Ed 2000, 38, 934.
16. Chuah, H. H. Polym Eng Sci 2001, 41, 308.
17. Huang, J. M.; Chang, F. C. J Appl Polym Sci 2002, 84, 850.
18. Kuo, Y. H.; Woo, E. M.; Kuo, T. Y. Polym J 2001, 33, 920.
19. Park, I.; Barlow, J. W.; Paul, D. R. J Polym Sci Polym, Phys Ed 1992, 30, 1021.
20. Sundararaj, U.; Macosko, C. W. Macromolecules 1995, 28, 2647.
21. Olabisi, O. Handbook of Thermoplastics; Marcel Dekker: New York, 1996; p 21.
22. Maa, C. T.; Chang, F. C. J Appl Polym Sci 1993, 49, 913.
23. Chang, D. Y.; Kuo, W. F.; Chang, F. C. Polym Networks Blends 1994, 4, 157.
24. Chiang, C. R.; Chang, F. C. J Appl Polym Sci 1996, 61, 2411.
25. Ibbett, R. N. NMR Spectroscopy of Polymers; Blackie Academic and Professional: London, 1993.
26. Mathias, L. J. Solid State NMR of Polymers; Plenum Press: New York, 1988.
27. Stejskal, E. O.; Schaefer, J.; Sefcik, M. D.; Mckay, R. A. Macromolecules 1981, 14, 275.
28. Natansohn, A. Polym Eng Sci 1992, 32, 1711.
29. Wang, J.; Cheung, M. K.; Mi, Y. Polymer 2001, 42, 2077.
30. Hill, D. J. T.; Whittaker, A. K.; Wong, K. W. Macromolecules 1999, 32, 5285.